nature climate change

SUPPLEMENTARY INFORMATION

https://doi.org/10.1038/s41558-019-0647-x

In the format provided by the authors and unedited.

The fate of Madagascar's rainforest habitat

Toni Lyn Morelli[1,2,26], Adam B. Smith[3,26], Amanda N. Mancini[4,5], Elizabeth A. Balko[6,7], Cortni Borgerson[8,9], Rainer Dolch[10], Zachary Farris[11], Sarah Federman[12], Christopher D. Golden[9,13], Sheila M. Holmes[14], Mitchell Irwin[15], Rachel L. Jacobs[16,25], Steig Johnson[14], Tony King[17,18], Shawn M. Lehman[19], Edward E. Louis Jr[20], Asia Murphy[21], Hery N. T. Randriahaingo[17], H. L. Lucien Randrianarimanana[17], Jonah Ratsimbazafy[22], Onja H. Razafindratsima[23] and Andrea L. Baden[4,5,24]*

[1]US Geological Survey, Department of Interior Northeast Climate Adaptation Science Center, Amherst, MA, USA. [2]Department of Environmental Conservation, University of Massachusetts, Amherst, MA, USA. [3]Center for Conservation and Sustainable Development, Missouri Botanical Garden, Saint Louis, MO, USA. [4]Department of Anthropology, The Graduate Center of the City University of New York, New York, NY, USA. [5]The New York Consortium in Evolutionary Primatology, New York, NY, USA. [6]Department of Biology, SUNY Oswego, Oswego, NY, USA. [7]Center for Teaching Innovation, Cornell University, Ithaca, NY, USA. [8]Department of Anthropology, Montclair State University, Montclair, NJ, USA. [9]Madagascar Health and Environmental Research (MAHERY), Maroantsetra, Madagascar. [10]Association Mitsinjo, Maroantsetra, Madagascar. [11]Department of Health and Exercise Science, Appalachian State University, Boone, NC, USA. [12]Department of Ecology and Evolutionary Biology,Yale University, New Haven, CT, USA. [13]Department of Nutrition, Harvard T. H. Chan School of Public Health, Boston, MA, USA. [14]Department of Anthropology and Archaeology, University of Calgary, Calgary, Alberta, Canada. [15]Department of Anthropology, Northern Illinois University, DeKalb, IL, USA. [16]Center for the Advanced Study of Human Paleobiology, Department of Anthropology, The George Washington University, Washington, DC, USA. [17]The Aspinall Foundation, Antananarivo, Madagascar. [18]The Aspinall Foundation, Port Lympne Reserve, Hythe, UK. [19]Department of Anthropology, University of Toronto, Toronto, Ontario, Canada. [20]Omaha's Henry Doorly Zoo and Aquarium, Omaha, NE, USA. [21]Department of Ecosystem Science and Management and the Huck Institutes of the Life Sciences, Pennsylvania State University, University Park, PA, USA. [22]Groupe d'Etude et de recherche sur les Primates de Madagascar, Antananarivo, Madagascar. [23]Department of Natural Resource Management, South Dakota State University, Brookings, SD, USA. [24]Department of Anthropology, Hunter College of the City University of New York, New York, NY, USA. [25]Present address: US Fish and Wildlife Service, National Fish and Wildlife Forensics Laboratory, Ashland, OR, USA. [26]These authors contributed equally: Toni Lyn Morelli, Adam B. Smith. *e-mail: andrea.baden@hunter.cuny.edu

The fate of Madagascar's rainforest habitat

Toni Lyn Morelli, Adam B. Smith, Amanda N. Mancini, Elizabeth A. Balko, Cortni Borgerson, Rainer Dolch, Zachary Farris, Sarah Federman, Christopher D. Golden, Sheila Holmes, Mitchell Irwin, Rachel L. Jacobs, Steig Johnson, Tony King, Shawn Lehman, Edward E. Louis, Jr., Asia Murphy, Hery N. T. Randriahaingo, H. L. Lucien Randrianarimanana, Jonah Ratsimbazafy, Onja H. Razafindratsima, Andrea L. Baden

Supplemental Methods and Results

Software

All analyses were conducted using code based on the dismo (Hijmans et al. 2017), raster (Hijmans 2017a), geosphere (Hijmans 2017b), and rgeos (Bivand & Rundel 2018) packages for the R Statistical Environment ver. 3.4.4 (R Core team 2018). The deforestation model also used the phcfM (Vieilledent 2013) and fasterRaster (Smith 2018) packages. The latter was linked to GRASS GIS 7.4.1 (Neteler et al. 2012). Ecological niche model (ENM) construction and evaluation procedures were conducted using the enmSdm package (Smith 2018). All code needed to reproduce the analysis is available at https://github.com/adamlilith/varecia.

Modeling forest cover

Madagascar has lost 44% of its forest cover since 1953 (Vieilledent et al. 2018) with little sign of abatement. In preliminary analyses we found that forest cover was a key variable defining the range of *Varecia*, which is corroborated by field studies which show that both species avoid forest loss (refs). Thus, owing to continued trends of deforestation and the sensitivity of *Varecia* to forests, we constructed a model of forest cover change following Vieilledent et al. (2013) using historical forest cover data from Vieilledent et al. (2018). For forest modeling we defined our study region as the entire extent of the eastern moist forest (to which *Varecia* are confined) using a mask for this ecoregion in Vieilledent et al. (2018—see their Figure 1) plus an additional buffer to account for the 12 *Varecia* survey sites (of 12,389) that fell outside this mask. We set the buffer width equal to the maximum distance (5803 m) between any *Varecia* occurrence and the nearest eastern moist forest multiplied by three. We modeled forest cover change within this region. All forest change modeling was conducted at 30-m spatial resolution using the Universal Transverse Mercator (UTM) geographic coordinate system.

Forest cover change models typically decompose the forest change process into amount of forest lost/gained and the location of loss/gain. Thus, the first part of the model estimated the amount of forest (here measured as land area) lost to deforestation (there is almost no gain in natural forest on Madagascar; Vieilledent et al. 2013). In most studies amount lost is expressed as a rate of change relative to extant forest (Puyravaud 2003). If rate is kept constant, then the total amount of forest removed in each time period will actually decline as the standing stock is reduced. Vieilledent et al. (2013) addressed this shortcoming by modeling deforestation rate as a function of human population density in subsections of Madagascar. Nonetheless, because rate is multiplied by total standing stock, assuming forest cover follows a compound loss trend (Puyravaud 2003) does not guarantee that the absolute amount of forest loss increases with population. Given this, a decision about the nature of deforestation must be made—does the total demand for forest products scale with population size independently of standing forest stock, or does diminished forest stock increase the cost of obtaining forest products and thus stimulate demand for imports or substitutes, possibly reducing total amount of forest consumed even if the rate of loss increases? Although there are few precedents on tropical forest insular systems, we note that the former (total demand scales independently of standing forest stock) seems to match trends observed for Haiti (Hedges et al. 2018) in which the amount of loss remained constant per time period until <1% of forest remained. As a result, we elected to model a deforestation amount (versus rate relative to standing stock) as a function of total population. Assuming that amount of forest removed in year t is given by aN_t where a is the per-capita rate of deforestation and N_t is total population size at time t. Then the total amount of forest lost over a given time period is

Eq. 1
$$D = aN_0 + aN_1 + aN_2 + aN_3 + aN_4 + ...$$
$$= a\sum N$$

Thus to estimate a we need only estimate total amount of forest lost and the sum of population across the time period. We used forest cover for 2000, 2005, 2010, and 2014 at a 30-m resolution from Vieilledent et al. (2018) who corrected layers from Hansen et al. (2013) to the remove plantations and “holes” in otherwise intact forest likely indicative of swidden agriculture. Using their data, we found that the annual amount of forest loss for eastern moist forest during the three

periods 2000-2005, 2005-2010, and 2010-2014 was 15.39, 14.38, and 25.22 m^2 per capita, respectively. If we set initial forest cover equal to the 2014 level (45,681 km2), assuming future loss trends follow the minimum rate (from 2005-2010), the entire eastern humid forest is predicted to be lost by 2077. Assuming the mean rate leads to complete loss by 2074, and assuming the maximum rate (from the most recent period) leads to complete loss by 2058. Since there was little difference between the mean and minimum rate in the year in which complete loss occurred, we elected to use an "optimistic" scenario in which continued forest loss followed the minimum (least loss) trend. Total amount lost per year was then estimated using estimates of Malagasy population for 2015-2080 obtained from the UN Population Division using "standard" projections of population growth rate (Raftety et al. 2013; United Nations 2017).

Following Vieilledent et al. (2013) we constructed a model of the location where forest loss was most likely in the eastern moist forest using spatial predictors including longitude, latitude, elevation and topographic slope, protected area (binary), distance to nearest settlement, distance to nearest road, distance to coast, distance to nearest major inland water body (rivers and lakes), distance to most recent deforestation, distance to forest edge, and forest fragmentation class (Riitters et al. 2000; calculated using a 5×5-moving window as per Vieilledent et al. 2013). Fragmentation class is based on two measures, "density" of forest in the window and degree of "connectivity" between adjacent cells in the window with forest cover. We used the GMTED2010 digital elevation model (Danielson & Gesch 2011) available at 7.5 arcsec resolution to represent elevation and slope. Location of protected areas was obtained from the World Database on Protected Area version 1.4 (IUCN & UNEP-WCWC 2018). Data on settlements, roads, and inland water bodies was sourced from DIVA-GIS (Hijmans et al. 2001) which serves data on settlements from the US National Geospatial Agency's Names Server (http://geonames.nga.mil/gns/html) and roads and inland water bodies from the Digital Chart of the World (Danko 1992; https://worldmap.harvard.edu/data/geonode:Digital_Chart_of_the_World). Distance to nearest deforestation event was calculated using deforestation in the prior period or year, and distance to forest edge using the forest edge in the prior period or year. To obviate problems arising from using predictors on very different scales we rescaled longitude and latitude to the range [-1, 1] and all distance-based metrics using $\log_{10}(x + 1)$.

To model deforestation location probability, we used the Bayesian variable-period logistic model (function deforestation) in the phcfM package (Vieilledent et al. 2018) for R (R Core Team 2018). Data on forest cover and loss in the periods 2005-2010 and 2010-2014 was used to train a preliminary model with all predictors (we could not use 2000-2005 with distance to deforestation as a predictor since there was not comparable data from a prior period). Forest loss/persistence (lack of loss) were obtained by randomly sampling 40,000 sites for each period across areas of the study region that were forested at the start of each period. We calculated variable importance by comparing the deviance of the null (intercept-only) model to deviance of a model with all variables except for the focal variable (Vieilledent et al. 2018). Following Vieilledent et al. (2013), we then inspected the signs of coefficients of each variable with an importance >0 and excluded any with signs that yielded counter-intuitive probabilities of deforestation. The final model used longitude, elevation, slope, protected area status, distance to nearest most recent deforestation event, and distance to nearest forest edge as predictors.

To project deforestation to the future we first calculated amount of forest lost, then removed forested pixels from the prior year's forest cover map such that the total number of pixels was within 1% of the estimated amount of forest to be lost. The location of this loss was identified using the probability of deforestation model (Supplemental Figure 1).

Niche overlap

We assessed overlap in the climatic niche of the two species using null model randomization tests (Warren et al. 2008; Broennimann et al. 2012) based on the four climatic variables used in the niche modeling. Niche overlap is computed by comparing the occupancy of environmental space (standardized by the frequency of available environmental space) of each species. Observed overlap is compared to a distribution of overlap values generated using a null model that randomizes the point locations across the study region. Specifically, we employed a flexible "rotate-translate-reflect" procedure (Nunes & Pearson 2017) to control for intra- and interspecific patterns in range geometry using the randPointsRespectingSelfOther2 function iterated 100 times using the family of randPointsBatch functions in the enmSdm package (Smith 2018). To achieve convergence we first thinned all occurrences such that the minimum pairwise distance between them was ≥ 17.5 km (*V.* variegata) or 8.75 km (*V. rubra*). Randomizations were required to have

a root-mean-square deviation from the observed spatial configuration of intra- and interspecific pairwise distances of ≤ 8.75 km. We used the combined set of all randomized ranges across all iterations to represent the background ("available") environment. Niche overlap was measured using Schoener's D and the Spearman rank-correlation coefficient (Dan Warren, personal communication).

Observed niche similarity between *V. variegata* and *V. rubra* was significantly greater than null expectation (Schoener's D statistic = 0.38, P = 0.03; rank correlation statistic = 0.97, P < 0.01).

Ecological niche modeling

We modeled the niche of each species and the genus (both species combined), then projected the niche to future climate and forest scenarios. Records of presence/non-detection were obtained from field expeditions conducted by the authors between 1989 and 2017 (Supplemental Table 6). All together we tallied 95 occurrences of *V. rubra* and 5882 of *V. variegata* (Supplemental Figure 2). Of these, 78% of occurrences of *V. rubra* and 98% of occurrences of *V. variegata* were obtained after 1999. Some of these occurrences represented repeat visits to the same or nearby locations, so we accounted for this in the modeling weighting scheme (see next section).

We performed several rounds of preliminary modeling to understand which predictors were most important in delimiting the range of *Varecia*. These tests included comparisons between: climate data sources (WORLDCLIM Version 2.0 versus CHELSA Version 1.2; Fick & Hijmans 2017; Karger et al. 2017), predictors including 7 climate predictors (temperature seasonality, mean temperature of the warmest quarter, mean temperature of the coldest quarter, mean annual precipitation, precipitation seasonality, precipitation of the wettest quarter, and precipitation of the driest quarter) and 7 predictors related to land cover, human disturbance and access, and topography (elevation, forest cover, forest loss, distance to forest cover loss, distance to nearest major road, distance to nearest major inland water body, and presence of humid forest biome), assuming either a narrow accessible area equal to just humid forest or broad accessible area equal to all of Madagascar for selection of background sites (Anderson & Raza 2010), and number of background sites (10,000 versus 100,000; Guevara et al. 2018). Based on these tests we chose a broad background characterized by 10,000 background sites with a limited set of predictors including four climate predictors from WORLDCLIM (mean temperature of the

warmest quarter, temperature seasonality, precipitation of the wettest quarter, and precipitation seasonality) and forest cover fragmentation class (Riiters et al. 2000; Vieilledent et al. 2013). All niche modeling was conducted at 30-arcsec spatial resolution. We resampled the climate layers to the 30×30-m resolution of the forest data using "nearest neighbor" interpolation. We note that this kind of interpolation does not change the values of the climate layers but simply "overlays" them onto the finer-scale grid and therefore the ENMs were trained using data at the original resolution of the raw data (30 arcsec for climate and 30×30 m for forest cover). WORLDCLIM climate layers for historical time periods represent interpolated climate data based on measurements from nearby weather stations plus topographical covariates and satellite-based sensor data (Fick & Hijmans 2017).

Ecological Niche Modeling: Bias correction

We addressed bias in search effort by using inverse p-weighting of presence sites (Stolar & Nielsen 2015). In particular we were concerned about the effect of spatial autocorrelation at fine scales arising from surveyors walking to nearby sites but distinguishing them as "independent." For example, if we just count 30-arcsec cells of the climate predictors that are known to be occupied then there were 335 occurrences of *V. variegata* and 40 of *V. rubra*. Hence, we down-weighted the influence of each presence site relative to its proximity to nearby sites (regardless of whether the nearby sites had a recorded presence or absence). To construct weights for presence sites we first estimated the characteristic distance of spatial autocorrelation between survey sites and compared it to random expectation. Specifically, we first calculated the pairwise distance between all survey sites (ignoring distances from a site to itself but including distances to the same site sampled multiple times). We then constructed a histogram of the frequency of distances using overlapping bins of 20 km width. The observed distribution was then compared to the distribution of pairwise distances sampled from randomly located sites sampled such that there were the same number of randomly located sites as in the actual survey dataset. We repeated the random sampling 100 times to create an envelope of null distance distributions. The characteristic distance of autocorrelation was then the smallest distance at which the observed frequency of distances fell below the 95^{th} quantile of the random distribution of distances (1-tailed test).

We found that survey sites had neighboring survey sites more frequently than expected at distances up to 70 km (Supplemental Figure 3). We ignored cases where the observed distribution fell above the 95th quantile in distance bins larger than the smallest bin because they coincided with suspected real breaks in the distribution of the species. To weight presence sites relative to one another we reasoned that two surveys at the same coordinate location should each be assigned a weight of 1/2, three such sites should each be assigned 1/3, and so on. We also reasoned that a site > 70 km from any other survey site was likely "independent" so should receive a weight of 1. Between these two extremes we assigned weights based on a linear trend between the points defined by 1 / (n + 1) where n is the number of neighboring survey sites within 0 and 70 km. Thus the effective number of neighbors for a given survey site was given by

Eq. 2 $$n_{eff} = \sum(1 - (d^* - d) / d^*)$$

where d^* is the characteristic distance of spatial autocorrelation between survey sites (70 km), and d is the distance between a neighbor and the focal site. The weight assigned to a presence was then

Eq. 3 $$(1 + n_{eff}) / (1 + n)$$

Background sites were initially assigned a weight of 1 (Stolar and Nielsen 2015), but for model training and evaluation we re-scaled weights for presence and background sites so the sum of weights of each class was equal (Maggini et al. 2006).

Ecological Niche Modeling: Model Training

To avoid complications interpreting models when they are projected outside the range of the training data (Anderson 2013; Merow et al. 2014) we chose models that tend to extrapolate in a dependable manner: generalized linear models (GLMs) and natural splines (NSs). GLMs parameterized with low-order terms tend to produce easily interpretable responses within and beyond the range of training data. Similarly, NSs extrapolate in a linear fashion beyond the range of the training data but are potentially more flexible than GLMs within the range (Hastie et al. 2009 Ch. 5). We used a step-wise procedure to construct the GLMs. In the first step we calculated models using each predictor (linear only, quadratic, two-way interactions), ranking these models using AIC_C, then constructing a "full" model based from top set of terms while

ensuring that there were at least 10 presence sites per coefficient needed to be estimated (excluding the intercept). We then calculated all possible models from these sets of terms (while respecting marginality) and selected the models with the lowest AIC_c. We used Firth's correction (Heinze 2006) to address issues related to complete separability. NSs were constructed in a similar manner. As described, we drew randomly located background sites from across Madagascar. Since *Varecia* are found only in the eastern moist forest, background sites that fell outside the eastern moist forest were assigned a forest fragmentation class of 0 (no forest) even if they fell in an otherwise forested area.

Ecological Niche Modeling: Model Evaluation

For model assessment we divided the range of each taxon into three mutually exclusive geographic areas (Boria et al. 2014). For *V. variegata* these comprise all presences north of latitude -17.20, south of -19.67, and presences between these two. For the genus we used the same scheme but with cutoff latitudes of -16.06 and -19.61. For *V. rubra* we divided the range using partitioning around medoids (function geoFold in the enmSdm package; Smith 2018) while ensuring that each fold had at least 15 presence sites. Background sites were assigned to the same fold as the nearest presence. Model performance was evaluated using a weighted Continuous Boyce Index which represents the correlation between model output and the actual probability of presence (Boyce et al. 2002; Hirzel et al. 2006). Models were trained on two of the geographic subsets for each species then tested against the training set and against the withheld set; the training and test sets were then rotated. We also trained an "all-sites" model using all presence sites for each species. From the best set of cross-validated models we used the associated all-sites model to project vulnerability to climate and habitat change into the future.

Ecological Niche Modeling: Future Climate and Forest Cover Scenarios

We used WORLDCLIM Version 1.4 (Hijmans et al. 2005) future climate layers for the period 2041 to 2060 and 2061 to 2080 (hereafter "2050s" and "2070s") for the RCP 2.6, 4.5, 6.0 and 8.5 emissions scenarios. WORLDCLIM climate layers for future projections are generated using the "delta" method wherein coarse-scale predictions from earth system models are first interpolated to the finer "target" resolution, then the difference between their predictions and the present-day downscaled predictions are added to present-day downscaled climate layers (Hijmans et al.

2005). There were 10 earth system models with projections for each period (including an ensemble prediction) available for these scenarios. To capture the full range of response of *Varecia* to projected climate change, we chose five that predicted the greatest difference in the selected climate predictors between the present and 2061-2080 under the RCP8.5 emissions scenario across 30-arcsec cells known to be occupied by the genus. For each variable the most extreme models were: temperature seasonality change ranging from -10.31 using the CCSM4 earth system model to +23.12 using HadGEM2-ES; mean temperature of the warmest quarter increasing by +4.07°C using IPSL-CM5A-LR (no models predicted a decrease); precipitation seasonality changing by +21.86 using HadGEM2-ES (none predicted a decrease); and precipitation of the wettest quarter changing by -86.9 mm using GISS-E2-R to +141.3 mm using BCC-CSM1-1. We used the predicted forest fragmentation class layer from the years 2050 and 2070 for the two "future" fragmentation class layers. We explored the relative effects of climate change versus deforestation by making predictions to future scenarios assuming: 1) no climate change (using present climate) but with deforestation; 2) no deforestation (using the 2014 forest cover layer) but with climate change; and 3) with both deforestation and climate change.

Ecological Niche Modeling: Results

The performance of the ENMs varied across taxa and between algorithms (Supplemental Table 4). GLMs for the genus had good calibration accuracy and were the highest and least variable across cross-validation folds (0.76 ± 0.08; mean ± sd). GLMs for *V. variegata* had similar performance to the genus but were more variable, while GLMs for *V. rubra* had poor and highly variable performance. For each taxon the NS models had lower performance with high variation across cross-validation folds. Owing to the poor and variable performance of the NS models hereafter we focus on the GLM ENMs.

Each taxon (each species and the genus) responded similarly to the climate predictors. The GLM trained on all presence sites produced response curves that increased in response to temperature seasonality and precipitation of the wettest quarter and declined in response to warmest quarter temperature and precipitation seasonality (Supplemental Figures 4-6). The genus and *V. variegata* responded similarly to forest fragmentation class; suitability increased as forest conditions approached "interior" conditions. Forest fragmentation class was not an important

variable in the all-sites *V. rubra* model (Supplemental Figure 5). For individual variables the average future values for each climate variable across current occurrence locations were well within the range of the training data (Supplemental Figures 4-6).

Based on these results, the fact that the two species have a highly similar niche, and that the species are largely separated by a riverine network that otherwise does not seem divide ecologically distinct regions, we chose to use the GLM ENM for the genus to characterize the vulnerability of *Varecia* to climate change and forest loss and fragmentation.

Supplemental Table 1 Change in forest cover and interior forest. Values are rounded to the nearest 10 km^2.

Year	Protection	Forest (km^2)	Interior (km^2)
2014	-	45,680	30,220
2050	relaxed	25,920	19,560
2050	strict	29,800	22,530
2070	relaxed	7,490	5,580
2070	strict	23,500	18,710

Supplemental Table 2 Deforestation model coefficients. Positive coefficient indicates that a higher value of the variable corresponds to higher likelihood of deforestation.

Model term	Coefficient (± SD)
Longitude (rescaled to [-1, 1])	-0.1551 ± 0.0358
Elevation (divided by 100)	0.3101 ± 0.0047
Topographic slope (degrees)	0.0221 ± 0.0026
Protected area (1 = protected, 0 = otherwise)	-0.5030 ± 0.0488
log10(distance to most recent deforestation in km)	-1.2201 ± 0.0482
log10(distance to nearest forest edge in km)	-0.7543 ± 0.0513

Supplemental Table 3 Sampling of *Varecia* (MS Excel File)

Supplemental Table 4 Performance of ecological niche models for each taxon (*V. variegata* and *V. rubra* and the both species together. Values represent the Continuous Boyce Index (CBI) calculated using either a rank correlation coefficient (Spearman) or parametric correlation coefficient (Pearson). GLM: generalized linear model; NS: natural splines.

Taxon	Algorithm	CBI ± SD
genus	GLM	0.76 ± 0.08
genus	NS	0.49 ± 0.48
V. rubra	GLM	-0.30 ± 0.59
V. rubra	NS	0.33 ± 0.68
V. variegata	GLM	0.74 ± 0.20
V. variegata	NS	0.36 ± 0.16

Supplemental Table 5 Mean Predicted Suitability by Scenario and Elevational Band (MS Excel File)

Supplemental Table 6 Change in Suitability by Protected Area (MS Excel File)

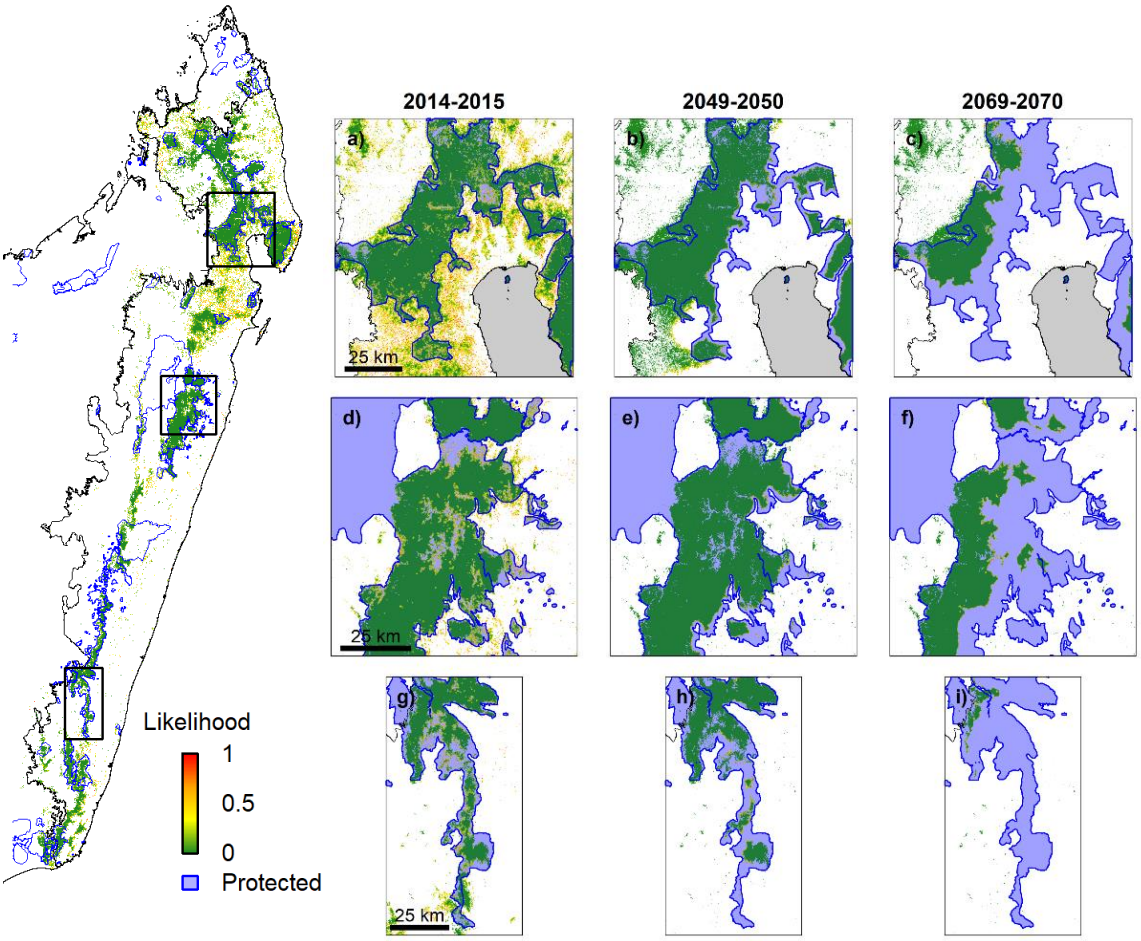

Supplemental Figure 1 The relative likelihood of deforestation across 2014-2015, 2049-2050 and 2069-2070. The leftmost map shows the likelihood of deforestation from 2014 to 2015, and the rectangles on the right represent likelihood of deforestation for 2014-2015, 2049-2050, and 2069-2070. The gray area in the Makira (northernmost) inset represents Helodrano Antongila Bay. The black outline within Madagascar encompasses the eastern moist forest ecoregion (Vieilledent et al. 2018). The relative likelihood of deforestation was highest near forest edges, areas of prior deforestation, outside protected areas, at lower elevations, and in more northern parts of the eastern moist forest.

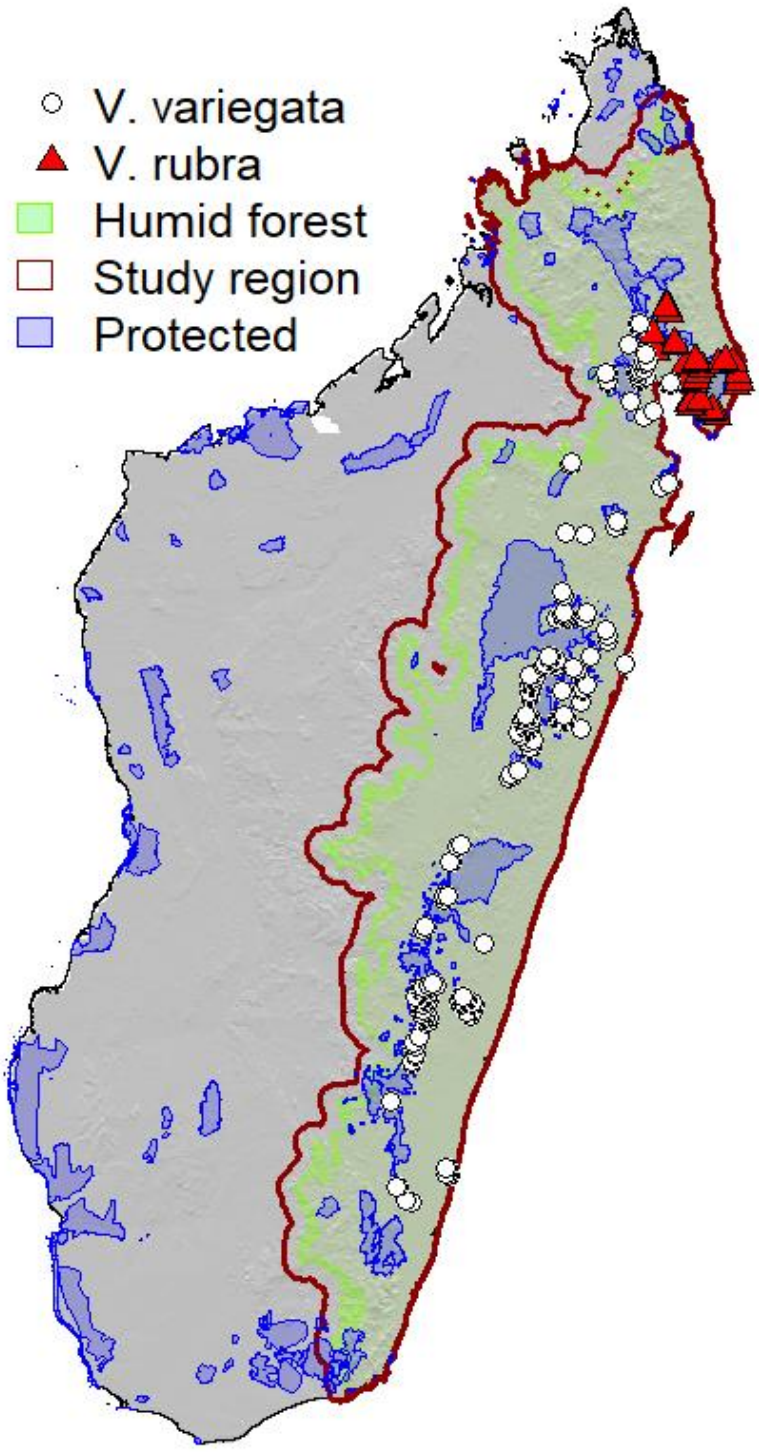

Supplemental Figure 2 Occurrence sites of *Varecia rubra* and *V. variegata*. The study region comprised the eastern moist forest plus a buffer of 17490 m to encompass all survey sites.

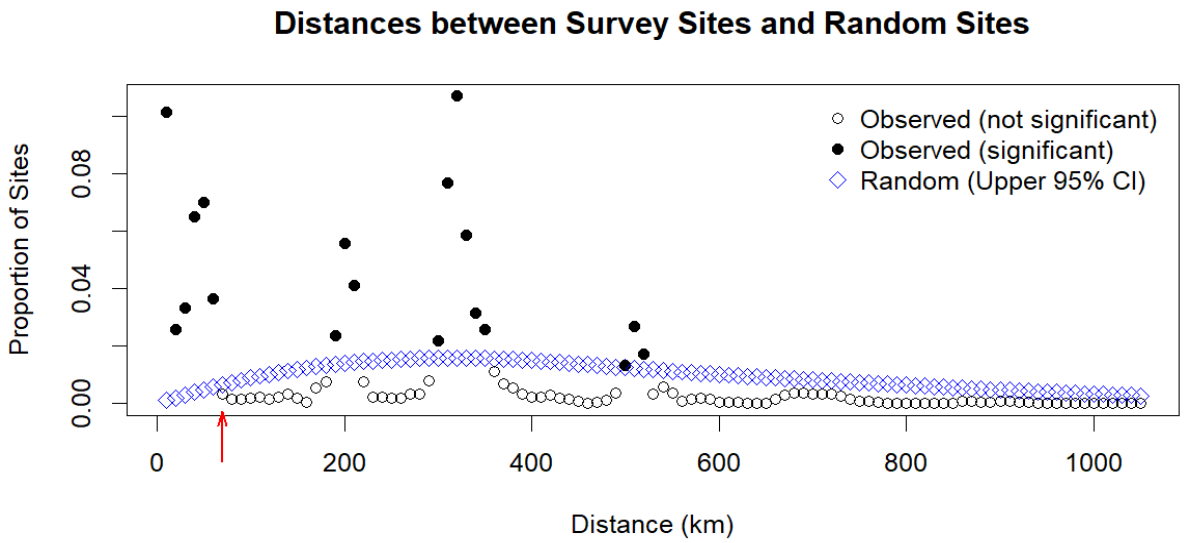

Supplemental Figure 3 Estimating the characteristic distance of spatial autocorrelation between survey sites. The x-axis represents the mid-point of overlapping bins 20 km wide. The y-axis is proportion of survey sites or of randomly located sites that had inter-point distances in each bin. For small distances the observed frequency of survey sites is much larger than the expected frequency based on random location of sites. The observed frequency first falls under the 95th quantile at 70 km (red arrow), the characteristic distance of spatial autocorrelation in survey sites. This distance was used to weight presence sites in ecological niche modeling. Occurrences farther apart than 70 km to their nearest neighbor received full weight and occurrences closer than this received reduced weight.

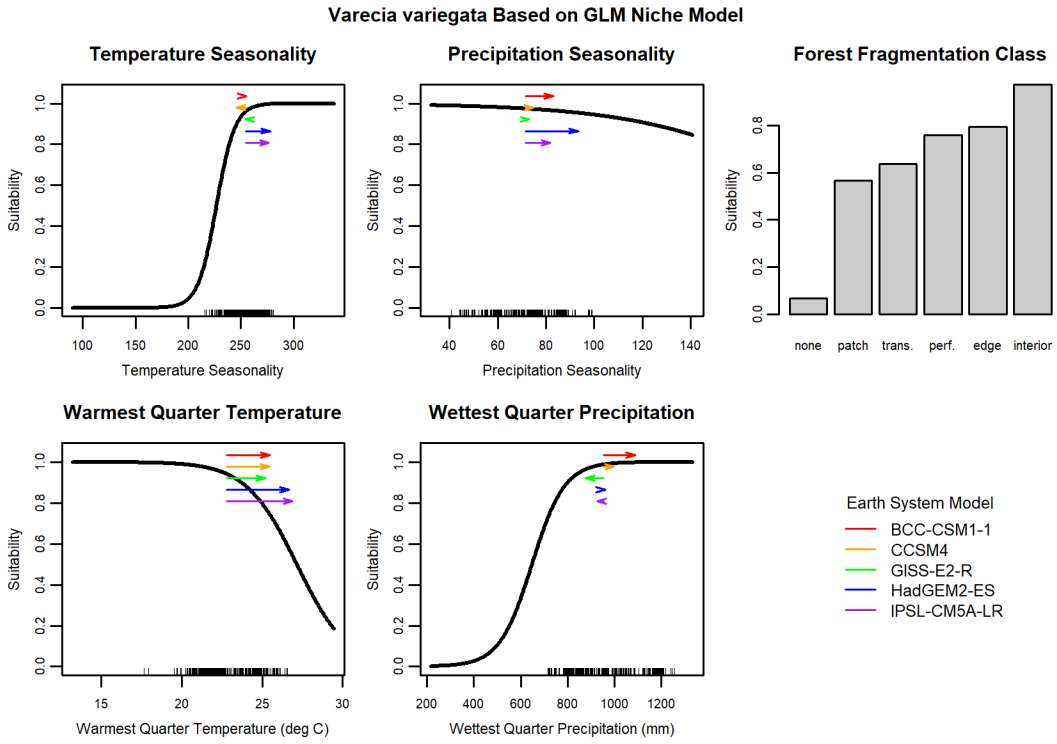

Supplemental Figure 4 Marginal change in environmental suitability as a function of each variable in the model for ***V. variegata***. The value of the focal variable was varied across the range of each variable currently observed in Madagascar with all other variables held at the median value across known presence sites (for the climatic variables forest fragmentation class was assumed to be "interior"). The rug plot along the x-axis indicates sites of known presence after duplicate occurrences in 30-arcsec cells were eliminated. The colored arrows represent the mean change in each variable across non-duplicate occurrence sites from current conditions to conditions expected by the 2070s under RCP8.5 for each variable at known occurrence locations of *V. variegata*. Forest fragmentation classes: no forest ("none", patch, edge, transitional ("trans."), perforated ("perf."), and interior.

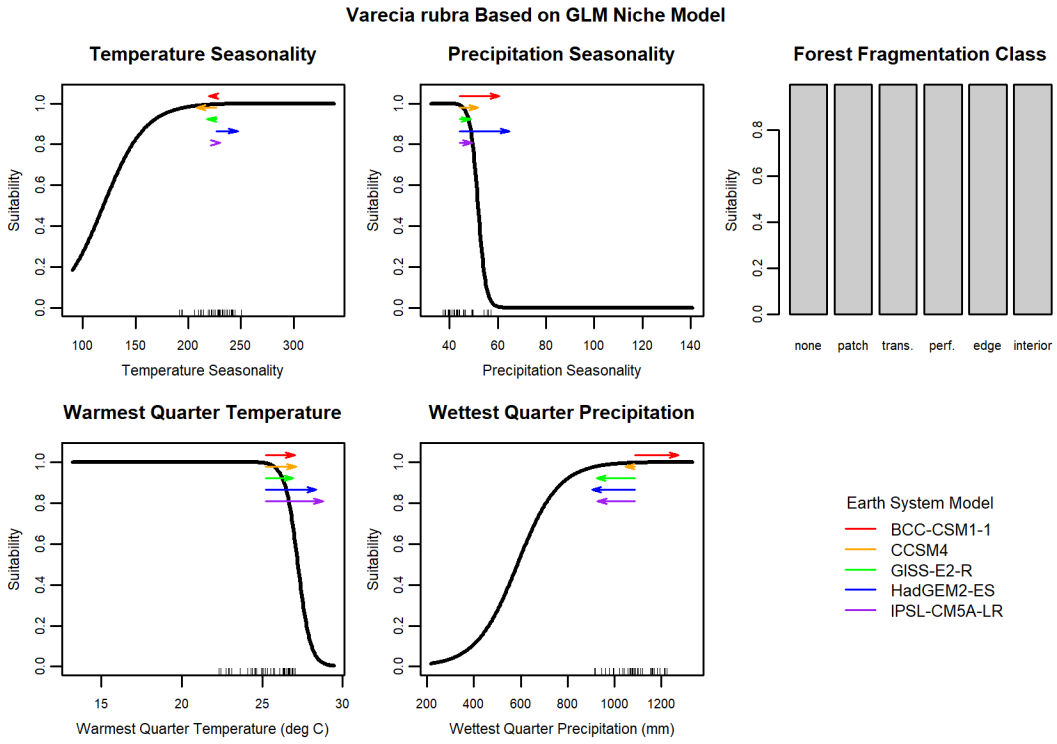

Supplemental Figure 5 Marginal change in environmental suitability as a function of each variable in the model for ***V. rubra***. The value of the focal variable was varied across the range of each variable currently observed in Madagascar with all other variables held at the median value across known presence sites (for the climatic variables forest fragmentation class was assumed to be "interior"). The rug plot along the x-axis indicates sites of known presence after duplicate occurrences in 30-arcsec cells were eliminated. The colored arrows represent the mean change in each variable across non-duplicate occurrence sites from current conditions to conditions expected by the 2070s under RCP8.5 for each variable at known occurrence locations of *V. rubra*. Forest fragmentation classes: no forest ("none", patch, edge, transitional ("trans."), perforated ("perf."), and interior.

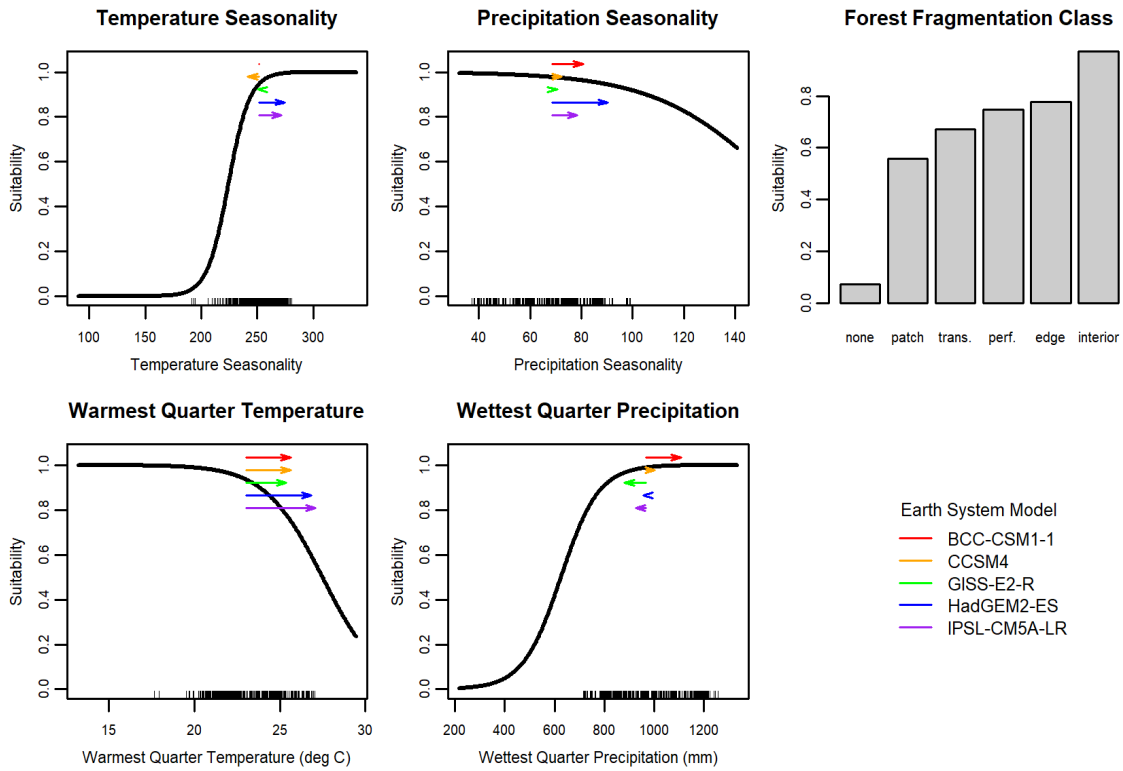

Supplemental Figure 6 Marginal change in environmental suitability as a function of each variable in the **genus**-level model. The value of the focal variable was varied across the range of each variable currently observed in Madagascar with all other variables held at the median value across known occupied sites (for the climatic variables forest fragmentation class was assumed to be "interior"). The rug plot along the x-axis indicates sites of known detections after duplicate occurrences in 30-arcsec cells were eliminated. The colored arrows represent the mean change in each variable across non-duplicate occurrence sites from current conditions to conditions expected by the 2070s under RCP8.5 for each variable at the genus' known occurrence locations. Forest fragmentation classes: no forest ("none"), patch, edge, transitional ("trans."), perforated ("perf."), and interior.

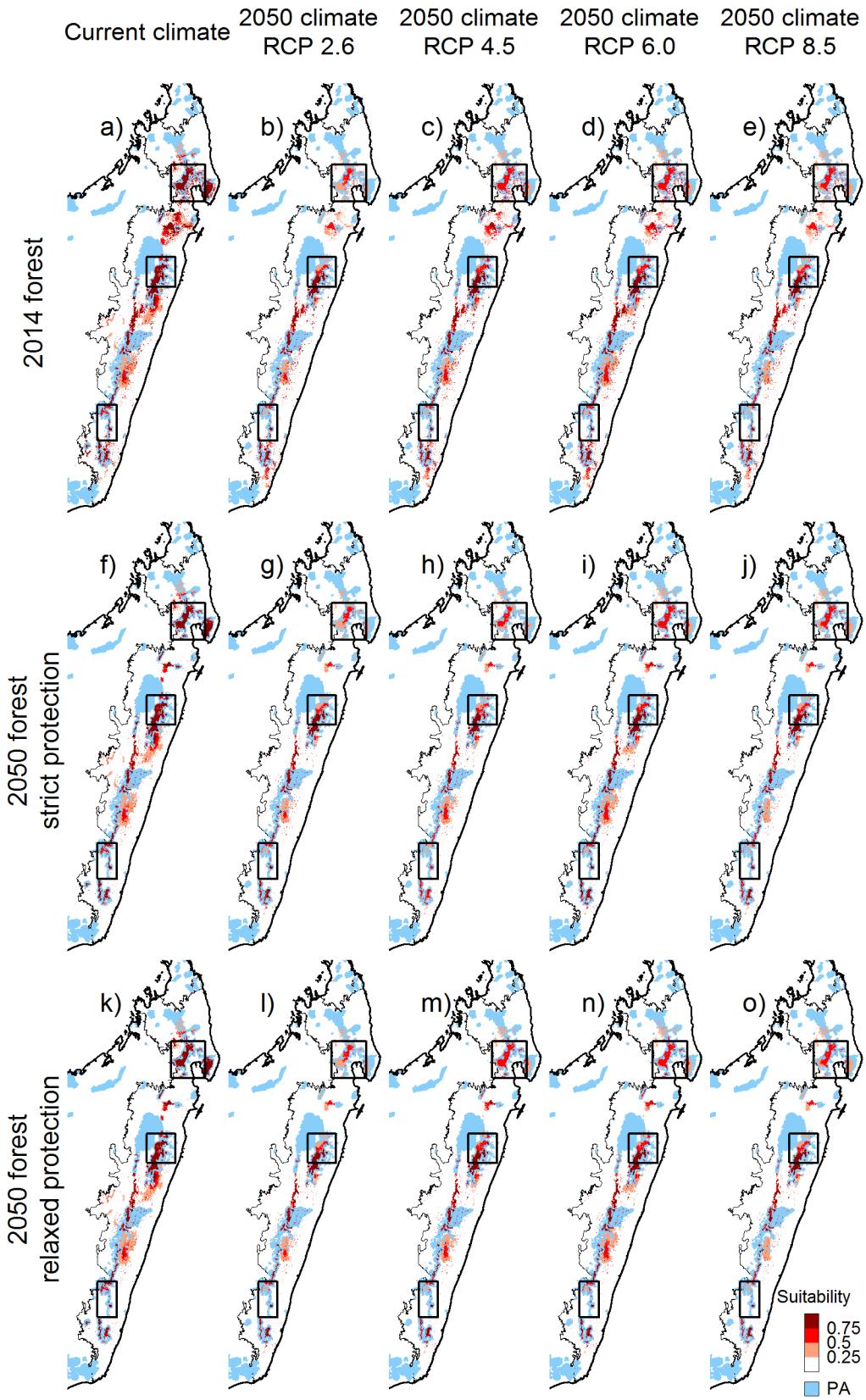
Current climate
2050 climate RCP 2.6
2050 climate RCP 4.5
2050 climate RCP 6.0
2050 climate RCP 8.5
2014 forest
2050 forest strict protection
2050 forest relaxed protection
a)
b)
c)
d)
e)
f)
g)
h)
i)
j)
k)
l)
m)
n)
o)
Suitability
0.75
0.5
0.25
PA

Supplemental Figure 7 Environmental suitability for *Varecia* for the current period and the **2050s**. The top left panel shows suitability given current climate and forest cover. The remainder of the top row shows the effect of climate change by the 2050s while holding forest at its current cover. The left column displays the effect of deforestation on suitability while climate is held at its current state. The remainder of the panels show combinations of deforestation and climate change. The three rectangles circumscribe areas highlighted in other figures. For climate change scenarios results are the average prediction across the 5 earth system models.

Literature cited

Anderson, R.P. 2013. A framework for using niche models to estimate impacts of climate change on species distributions. Annals of the New York Academy of Sciences 1297:8-28.

Anderson, R.P. and A. Raza. 2010. The effect of the extent of the study region on GIS models of species geographic distributions and estimates of niche evolution: Preliminary tests with montane rodents (genus *Nephelomys*) in Venezuela. Journal of Biogeography 37:1378-1393.

Bivand, R. and Rundel, C. 2018. rgeos: Interface to Geometry Engine - Open Source ('GEOS'). R package version 0.3-28. https://CRAN.R-project.org/package=rgeos

Boria, R.A., Olson, L.E., Goodman, S.M., and Anderson, R.P. 2016. A single-algorithm ensemble approach to estimating suitability and uncertainty: Cross-time projections for four Malagasy tenrecs. Diversity and Distributions 23:196-208.

Boyce, M.S., Vernier, P.R., Nielsen, S.E., and Schmiegelow, F.K.A. 2002. Evaluating resource selection functions. Ecological Modeling 157:281-300.

Broennimann, O., Fitzpatrick, M.C., Pearman, P.B., Petitpierre, B., Pellissier, L., Yoccoz, N.G., Thuiller, W., Fortin, M-J., Randin, C., Zimmermann, N.E., Graham, C.H., and Guisan, A. 2012. Measuring ecological niche overlap from occurrence and spatial environmental data. Global Ecology and Biogeography 21:481-497.

Danielson, J.J. and Gesch, D.B. 2011. Global multi-resolution terrain elevation data 2010 (GMTED2010). US Geological Survey Open-File Report Series 2011-1073. doi: 10.3133/ofr20111073

Danko, D.M. 1992. The digital chart of the world project. Photogrammetric Engineering & Remote Sensing 58:1125-1128.

Fick, S.E. and R.J. Hijmans, 2017. Worldclim 2: New 1-km spatial resolution climate surfaces for global land areas. International Journal of Climatology 37:4302-4315.

Guevara, L., Gerstner, B.E., Kass, J.M., and Anderson, R.P. 2018. Toward ecologically realistic predictions of species distributions: A cross-time example from tropical montane cloud forests. Global Change Biology 24:1511-1522.

Hansen, M.C., Potapov, P.V., Moore, R., Hancher, M., Turubanova, S.A. Tyukavina, A., Thau, D., Stehman, S.V., Goetz, S.J., Loveland, T.R.., Kommareddy, A.,. Egerov A., Chini, L.,

Justice, C.O., and Townshend, J.R.G. 2013. High-resolution global maps of 21st-century forest cover change. Science 342:850-853.

Hastie, T., Tibshirani, R., and Friedman, J. 2009. The Elements of Statistical Learning: Data Mining, Inference, and Prediction. Springer, New York.

Heinze, G. 2006. A comparative investigation of methods for logistic regression with separated or nearly separated data. Statistics in Medicine. 25:4216-4226.

Hijmans, R.J. 2017a. raster: Geographic Data Analysis and Modeling. R package version 2.6-7. https://CRAN.R-project.org/package=raster

Hijmans, R.J. 2017b. geosphere: Spherical Trigonometry. R package version 1.5-7. https://CRAN.R-project.org/package=geosphere

Hijmans, R.J., Cameron, S.E., Parra, J.L., Jones, P.G., and Jarvis, A. 2005. Very high resolution interpolated climate surfaces for global land areas. International Journal of Climatology 25:1965-1978.

Hijmans, R.J., Phillips, S., Leathwick, J., and Elith, J. 2017. dismo: Species Distribution Modeling. R package version 1.1-4. https://CRAN.R-project.org/package=dismo

Hirzel, A.H., Le Lay, G., Helfer, V., Randin, C., and Guisan, A. 2006. Evaluating the ability of habitat suitability models to predict species presences. Ecological Modeling 199:142-152.

IUCN and UNEP-WCMC. 2018. The World Database on Protected Areas (WDPA). Cambridge, UK: UNEP-WCMC. Available at: www.protectedplanet.net. Accessed 2018-10-08.

Karger, D.N., Conrad, O., Böhner, J., Kawohl, T., Kreft, H., Soria-Auza, R.W., Zimmermann, N.E., Linder, H.P. & Kessler, M. 2017 Climatologies at high resolution for the earth’s land surface areas. Scientific Data 4:170122.

Maggini, R., A. Lehmann, N.E. Zimmermann, and A. Guisan. 2006. Improving generalized regression analysis for the spatial prediction of forest communities. Journal of Biogeography 33:1729-1749.

Merow, C., Smith, M.J., Edwards, Jr., T.C., Guisan, A., McMahon, S.M., Normand, S., Thuiller, W., Wüest, R.O., Zimmermann, N.E., and Elith, J. 2014. What do we gain from simplicity versus complexity in species distribution models? Ecography 37:1267-1281.

Neteler, M., Bowman, M.H., Landa, M., and Metz, M. 2012. GRASS GIS: A multi-purpose open source GIS. Environmental Modeling and Software 31:124-130.

Nunes, L.A. and Pearson, R.G. 2017. A null biogeographical test for assessing ecological niche evolution. Journal of Biogeography 44:1331-1343.

Puyravaud, J-P. 2003. Standardizing the calculation of the annual rate of deforestation. Forest Ecology and Management 177:593-596.

Raftery, A.E., N. Li, H. Ševčíková, P. Gerland, and G.K. Heili. 2012. Bayesian probabilistic population projections for all countries. Proceedings of the National Academy of Sciences. 109:13915-13921.

Riitters, K., J. Wickham, R. O'Neill, B. Jones, and E. Smith. 2000. Global-scale patterns of forest fragmentation. Conservation Ecology 4:3. URL: http://www.consecol.org/vol4/iss2/art3/

Smith, A.B. 2018. enmSdm: Tools for modeling niches and distributions of species. R package version 0.3.4.1. http://www.github.com/adamlilith/enmSdm

Smith, A.B. 2018. fasterRaster: Faster raster processing in R using GRASS GIS. R package version 0.4.0. http://www.github.com/adamlilith/fasterRaster

Stolar, J. and Neilsen, S.E. 2015. Accounting for spatially biased sampling effort in presence-only species distribution models. Diversity and Distributions 21:595-608.

United Nations. 2017. World Population Prospects 2017. https://population.un.org/wpp/Download/Standard/Population/ (accessed 2018-10-01).

Vieilledent, G., Grinand, C., Rakotomala, F.A., Ranaivosoa, R., Rakotoarijaona, J-R., Allnutt, T.F., and Achard, F. 2018. Combining global tree cover loss data with historical national forest cover maps to look at six decades of deforestation and forest fragmentation in Madagascar. Biological Conservation 222:189-197.

Vieilledent, G., Grinand, C., and Vaudry, R. 2013. Forecasting deforestation and carbon emissions in tropical developing countries facing demographic expansion: A case study in Madagascar. Ecology & Evolution 3:1702-1716.

Warren, D.L., Glor, R.E., and Turelli, M. 2008. Environmental niche equivalency versus conservatism: Quantitative approaches to niche evolution. Evolution 62:2868-2883.